Scratch testing of ZrN coating on Ti-6Al-4V titanium alloy surface preliminary treated by compression plasma flows impact

N.N. Cherenda [1]*, A.B. Petukh [1], A.K. Kuleshov [1], D.P. Rusalsky [1], N.V. Bibik [1], V.V. Uglov [1], S.N. Grigoriev [2], A.A. Vereschaka[3], V.M. Astashynski [4], A.M. Kuzmitski [4]

[1]Belarusian State University, Nezavisimosti ave. 4, 220030 Minsk, Belarus;
[2]Moscow State University of Technology "STANKIN", Vadkovsky Lane 3a, 127055 Moscow, Russia;
[3]Institute of Design and Technological Informatics of the Russian Academy of Sciences (IDTI RAS), Vadkovsky Lane 18a, 127055 Moscow, Russia;
[4]A.V.Lykov Heat and Mass Transfer Institute of the National Academy of sciences of Belarus, P. Brovka str. 15, 220072 Minsk, Belarus;
*****Correspondence: Tel.: +375172095590; Fax: +3752095445; E-mail: cherenda@bsu.by

Abstract: Investigation of compression plasma flows preliminary impact influence on adhesion of ZrN coating deposited on Ti-6Al-4V titanium alloy was carried out in this work. Profilometry, X-ray diffraction, scratch-testing were used as investigation techniques. The findings showed that preliminary plasma impact led to the formation of developed surface relief and synthesis of titanium nitride on the surface of the alloy. Plasma processing provided a higher critical force Lc3 during scratch tests, which increases from 44 N (without processing) to 137 N (the density of absorbed energy 26 J/cm^2, 6 pulses). With a decrease in the density of absorbed energy and a growth of the number of pulses, there was a tendency of the critical force Lc3 increase, that is mainly associated with the formation of an intermediate layer δ-TiN during plasma impact, the thickness of which increased with a growth of the number of pulses and a decrease in the density of absorbed energy.

Keywords: titanium alloy; medical implants; coating; plasma; surface relief; friction coefficient; adhesion; scratch testing

1. Introduction

Ti-6Al-4V is one of the most widely used titanium alloy for orthopedic and dental applications (Brunello et al.; 2018). This alloy satisfies the main requirements for metallic implants: biocompatibility, corrosion resistance, suitable mechanical properties and good osseo-integration (Chen and Thouas, 2015). At the same time it contains potentially toxic atoms of aluminum and vanadium which have the risk of releasing into the human body (Chen and Thouas, 2015; Kaur and Singh, 2019; Chen et al., 2023). Protective coating formation on the surface of the implant is the common way to avoid this negative effect. Besides that coating deposition is an effective way to improve the tribological properties of biomedical titanium alloys (Zhao et al., 2021).
Adhesion of protective coatings to implants surface is strongly influenced by the surface roughness. In general, increase in the surface roughness should lead to the growth of interface area between coating and substrate and hence to the growth of number of bonds and growth of adhesion force (Croll, 2020). Adhesion force increase was observed e.g. in (Bruera, 2023) for cold-sprayed Cu particles deposited on stainless steel substrate with the growth of roughness up to a $R_z \sim 34$ μm. Similar tendency was found for WC-12Co coating on steel (Tahir et al., 2020). At the same time there are examples that increase of surface roughness resulted in coating adhesion decrease (Takadoum and Bennani, 1997; Bruera et al., 2023).
The scratch tests are widely used for measuring adhesion of coating to substrate (Bull and Berasetegui, 2006; Croll, 2020; Randall, 2019). In the typical test a diamond indenter generates a track on sample under constant or progressively increasing load. A combined investigations by optical microscopy, friction force, acoustic emission or determination of indenter penetration

depth allow to find some critical failure points or critical loads - Lc (Croll, 2020; Randall, 2019). Three main critical loads are usually determined: Lc1 corresponding to initial cracking appearance, Lc2 – first chipping and Lc3 – full delamination of a coating (Randall, 2019). Besides that this type of test can be used for determination of hardening parameters (Leroch et al., 2023), fracture toughness (Liu et al., 2023), investigation of abrasive wear (Varga et al., 2023) and plastic properties of metallic materials (Zhang et al., 2022).
A number of techniques have been used for implant surface modification to prevent bacterial attachment, enhance osseo-integration, increase mechanical and tribological properties, improve coating adhesion etc. (Nouri and Wen, 2015; Chouirfa et al., 2019; Wang et.al, 2020; Lu et al., 2020; Kurup et al., 2021; Herrera-Jimenez et al., 2021; Simões et al., 2023; Grabovetskaya et al., 2023; Wu et al., 2023; Sachin et al., 2022). Efficiency of surface relief modification was demonstrated in (Honget al., 2023; Caraguay et al., 2023) when plasma and laser pre-treatment of metal alloys provided coating adhesion improvement due to increasing of contact area between coating and substrate. Compression plasma flows (CPF) generated by quasi-stationary plasma accelerators can be also effectively used for modification of strength and tribological properties of steels (Uglov et al.; 2004; Cherenda et al., 2016) and decrease of toxic elements concentration at the surface of Ti-6Al-4V titanium alloy (Cherenda et al., 2018). In the previous work it was already shown that CPF treatment of Ti-6Al-4V titanium alloy resulted in substantial change of surface roughness and waviness parameters (Cherenda et al., 2024). Increase of pulses number led to the growth of R_a value from 0.4 μm up to 2.7 μm. R_a value corresponds to the roughness range providing best conditions for osseo-integration (Robles et al., 2023; Tardelli et al., 2022). The behavior of the waviness parameter W_a correlated with the behavior of R_a. Usage of nitrogen as plasma generating gas also led to the formation of titanium nitride with a cubic crystal lattice which prevents the development of the surface relief at the lowest density of energy absorbed by the surface (Cherenda et al., 2024).
Investigation of adhesion and tribological properties of protective ZrN coating deposited on the surface of Ti-6Al-4V alloy with different surface relief formed by preliminary CPF treatment was the main aim of this work. Zr-based nitride coatings possess good biocompatibility, wear and corrosion resistance, making them suitable candidates for tribological and biomedical applications (Ul-Hamid, 2021). Addition of Zr to TiN coating also improves its tribological behavior (Kumar and Mulik, 2023). Besides that ZrN based coating possesses better adhesion to high speed steel and WC-Co than TiN based coating (Vereschaka et al., 2018; Ward et al., 1996).

2. Experimental

The samples of Ti-6Al-4V titanium alloy (Grade 5) were used for investigations. The diameter of the samples was 25 mm, their thickness – 3 mm. The samples were mechanically grinded before plasma treatment. The parameters of the surface roughness and waviness were equal to: R_a=0.4 μm, R_z=4.1 μm, W_a= 0.24 μm. Roughness parameters of samples corresponded to roughness parameters of workpieces used for production of hip joints parts.
Compression plasma flows treatment of Ti-6Al-4V alloy surface was carried out before coating deposition. CPF were obtained using a gas-discharge quasi-stationary plasma accelerator: magneto-plasma compressor of compact geometry powered with the capacitive storage of 1200 mF, operating at the voltage of 4 kV. Nitrogen was used as a plasma-forming gas. The pressure in the pre-evacuated vacuum chamber was 10^{-3} Pa. The pressure of plasma-forming gas was 400 Pa. The discharge duration amounts to 100 μs. The density of energy absorbed by the surface layer (Q) of the target was changed in the range of 26-37 J/cm^2 per pulse (registered by calorimetric measurements). Treatment was carried out by 1-6 pulses (n) at the interval of 3-5 s.
ZrN coating was deposited by vacuum arc deposition technique with controlled movement of cathode spot from Zr cathode in nitrogen atmosphere (Grigoriev et al., 2023; Vereschaka et al., 2020). Cleaning of the surface by Zr ions was carried out before deposition resulting in formation of thin (~ 50 nm) metal sublayer. ZrN coating thickness was about 3 μm.

Surface topography was characterized using MahrSufr SD 26 profilometer. Six tracks were made on each of the sample. The length of the track was 17 mm, length of base line for calculation of roughness and waviness parameters was 5.7 mm. Each parameter was averaged after measurements on 6 tracks. The phase composition of the surface layer was investigated by means of the X-ray diffraction method using the Ultima IV RIGAKU diffractometer in Bragg-Brentano geometry with parallel beams in Cu Kα radiation. Scratch tests were carried out with 0.4 mm radius diamond indenter with a load linearly increasing from 0.05 to 140 N. The scratch tracks length was 15 mm (loading speed 0.17 kg/s, sample movement speed 0.19 mm/s) and 7.5 mm (loading speed 0.16 kg/s, sample movement speed 0.08 mm/s). Three tests were carried out on each sample.

3. Results and Discussion

The CPF impact on Ti-6Al-4V surface led to the formation of a more developed relief (Figure 1). Results of surface roughness and waviness parameters investigation received in the previous work (Cherenda et al., 2024) are summarized in Table 1. One can see that the increase in the number of pulses for Q=30-37 J/cm^2 led to the growth of roughness and waviness parameters value. It is well-known that impact of high temperature plasma flows is followed by surface layer melting. Acceleration of the melt due to impulse transfer from the plasma flow led to appearance of hydrodynamic instabilities at the plasma – melt border (Krasnikov et al., 2007; Bazylev et al., 2009; Astashinski et al., 2014). As a result the plasma-melt interface will changes it shape due to a sharp increase in the amplitude of initially small perturbations. Such perturbations begin to increase with time and, after crystallization, determine mainly the surface topography. With the growth of number of pulses each subsequent pulse is superimposed on a more developed surface created by the previous one, leading to the formation of more developed relief.

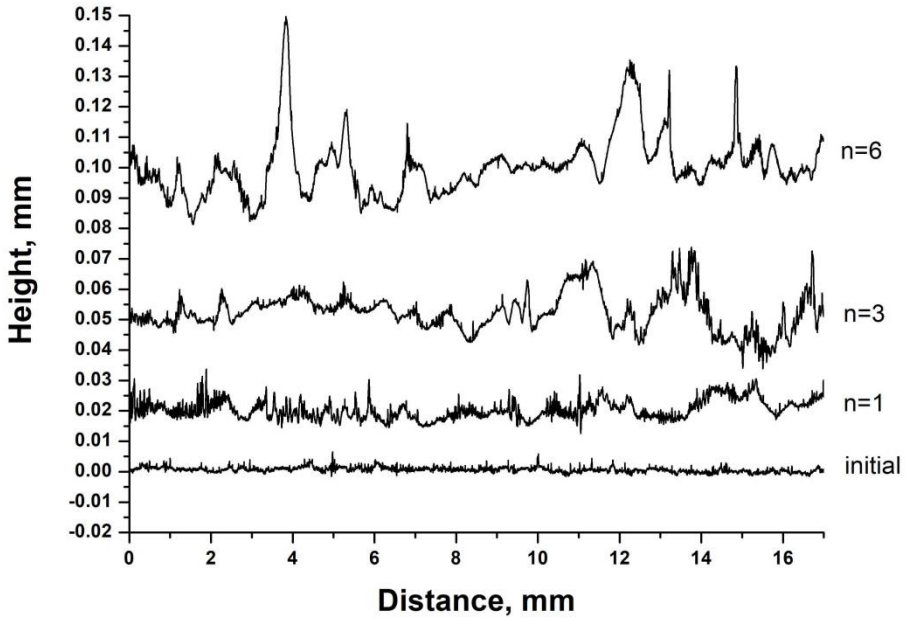

Figure 1. Surface profile of initial sample and samples treated at Q=30 J/cm^2 with 1-6 pulses.

During treatment with minimal Q value of 26 J/cm^2 R_a parameter as well as R_z parameter were diminished with the growth of the number of pulses, while W_a value was slightly increased in contrast to other treatment regimes. Such behavior is associated with a strong influence of TiN film formed on alloy surface.

Presence of nitrogen as a plasma forming gas in a vacuum chamber led to it interaction with the titanium alloy surface heated under plasma action (Cherenda et al., 2012). Due to high crystallization temperature of δ-TiN (~ 2930 ^{o}C) nitride film that can be formed on the surface of the melt will prevent development of melt perturbations. X-ray diffraction analysis confirmed the formation of δ-TiN (with cubic crystalline lattice) on the surface of the alloy (Figure 2). The diffraction peaks of both δ-TiN and α-Ti were shifted to the region of larger angles indicating formation of δ-Ti(Al,V)N and α-Ti(Al,V) solid solutions (Cherenda et al., 2024). Growth of the pulses number resulted in increase of nitride diffraction line intensity that was the evident of it higher volume fraction in the analyzed layer (formation of thicker nitride film). Analysis of diffraction pattern presented in Figure 2 showed that the nitride volume fraction diminished with the growth of the energy absorbed by the surface layer. In particular the ratio of the total intensity of the diffraction lines of titanium nitride (ΣI_{TiN}) to total intensity of the diffraction lines of titanium (ΣI_{Ti}) was equal to 0.30 at 26 J/cm^2, to 0.20 at 30 J/cm^2 and to 0.18 at 37 J/cm^2 after six plasma pulses. The main reasons for such behavior with a change in the number of pulses and the absorbed energy density were considered earlier (Cherenda et al., 2024).

a)

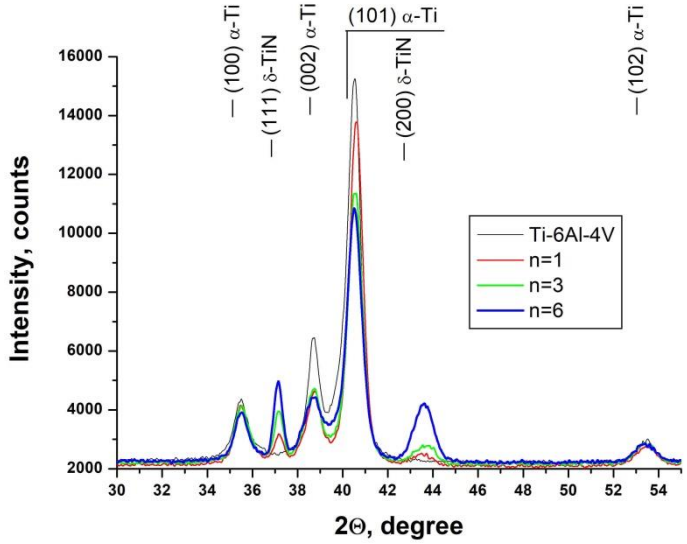

b)

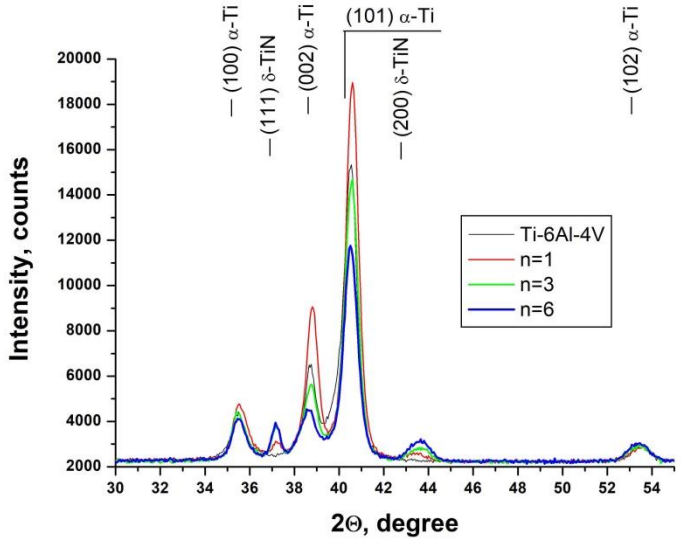

Figure 2. X-ray diffraction patterns of samples treated at 26 J/cm^2 (a) and 37 J/cm^2 (b) with different number of pulses.

Thus one can see that surface roughness and volume fraction (thickness) of δ-TiN were increased with the growth of the pulses number. Both of these factors can influence on adhesion of protective coating deposited on the alloy surface modified by plasma.
ZrN coating was deposited on the surface of the samples after preliminary plasma treatment Coated samples were tested using a scratch tester at a track length of 15 mm. Since the surface was characterized by developed roughness it was not possible to determine critical forces according to the acoustic sensor. That is why the dependence of the indenter friction coefficient along track length was analyzed (Figure 3). As it can be seen from the figure, the initial sample with coating had a sharp increase in the coefficient of friction at the length of the track corresponding to the complete delamination of the coating that was confirmed by the data of optical microscopy. For plasma pre-treated samples an increase in friction coefficient in the range of the track of 0-6 mm was observed. The oscillations of the friction coefficient were also visible on dependencies which were associated with the developed surface of the sample. This effect makes it difficult to determine the values of critical normal force by such a dependence. Therefore the determination of critical normal force was carried out with the help of optical microscopy only that can used for correct determination of Lc3 (Randall, 2019).

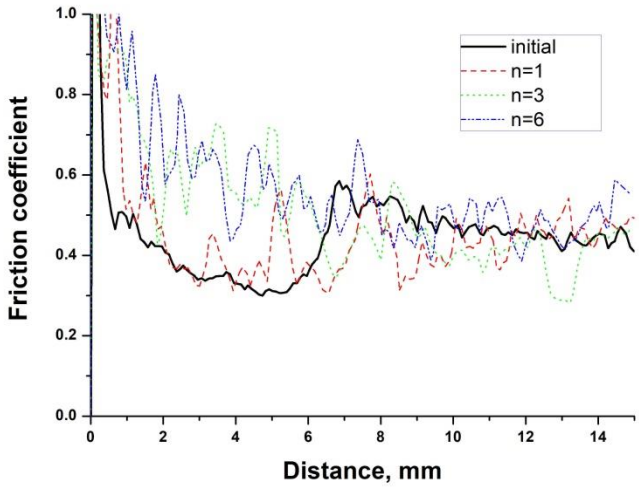

Figure 3. Dependence of friction coefficient on sliding distance of ZrN coating deposited on initial Ti-6Al-4V sample and on samples preliminary treated by CPF at 37 J/cm^2 with different number of pulses.

By means of optical microscopy investigations the distance from the beginning of the track was measured, on which the coating was fully removed. After that the corresponding load and normal critical force were determined using the calibration graph of the linear dependence of the applied mass on the length of the track. Findings have shown that in the original sample, the full removal of the coating was observed at the value of critical force Lc3=44 N (Figure 4). After that indenter mainly interacted with the surface of the alloy in the track and continuous delamination of the coating along the edges of the track was observed. A relatively developed surface in the original sample did not allow correctly determine Lc1 and Lc2 critical forces.

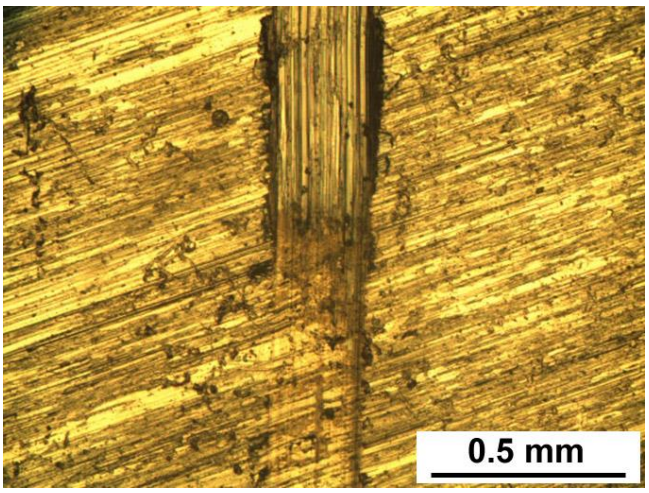

Figure 4. Optical microscopy image of scratch track on ZrN coated initial sample at the place of full removal of the coating.

On samples treated with CPF at Q = 37 J/cm^2, tracks were characterized by the formation of several sequential local areas at which the partial removal of the coating was observed and the last area, starting from which the indenter interacted directly with the alloy in the track and continuous delamination of the coating on the edges of the track was seen (Figure 5). The appearance of several areas was associated with a developed surface formed after plasma treatment. For the case presented in Figure 5, “peeling” areas corresponded to the normal force of 44 N, 57 N and 87 N.

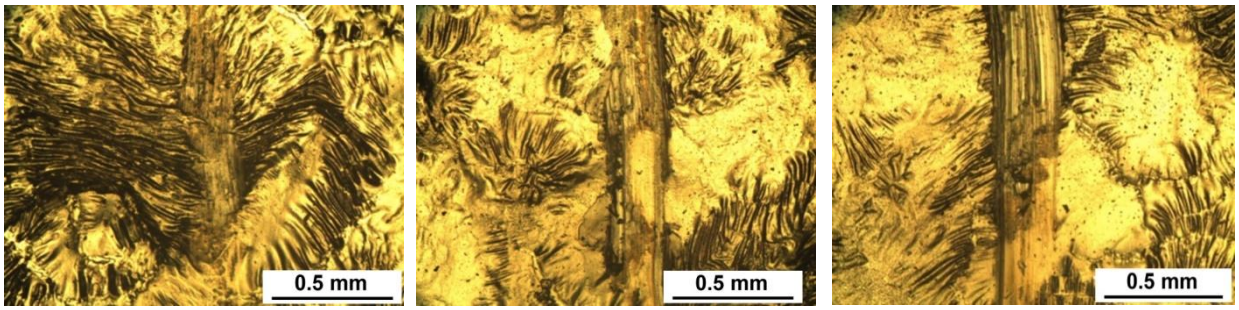

a *b* *c*

Figure 5. Optical microscopy images of scratch tracks on ZrN coated sample preliminary treated with Q = 37 J/cm^2 and n=6 pulses, at the length of the track: 6 mm (a), 8 mm (b) and 13 mm (c).

For all samples subjected to preliminary plasma treatment at Q = 37 J/cm^2, the 1st local area of coating removal was in the range of normal critical force 31 - 44 N, that was comparable to the result obtained on the initial sample with the coating. It should be noted that the critical tangential force reached at this normal load in plasma treated samples should be higher due to the more developed relief. So one can expect a higher adhesive strength of the coating deposited on such samples. The full removal of the coating was observed at the critical normal force of 81-88 N as a confirmation of higher adhesion strength.

The appearance of several areas of the coating removal was characteristic for all plasma treatment modes. The results of critical force Lc3 determination are summarized in Table 2. The critical force at which the 1st such area was observed was marked as$Lc3^{min}$, and a critical force, at which full coating removal occurred was marked as $Lc3^{max}$.

An analysis of the results presented in the table showed that preliminary treatment of the samples provided a higher value of the critical force Lc3 compared to that of untreated sample. With a decrease in the density of absorbed energy, there was a tendency of increase both $Lc3^{min}$ and

$Lc3^{max}$. A similar trend can be found with an increase in the number of pulses. However, these trends did not fully correspond to the dependencies obtained for the parameters of roughness and waviness (Table 1). For example, for the case of treatment at Q = 26 J/cm^2, a decrease in the parameters R_a and R_z and increase in Lc3 with the growth of the number of pulses were observed. Treatment at the density of absorbed energy Q = 37 J/cm^2 provided the formation of a more developed surface relief than treatment at Q = 26 J/cm^2, while the value of Lc3 for the case of Q = 37 J/cm^2 was less. Some investigations of other authors (Takadom and Bennani, 1997; Bruera et al., 2023) showed that increase of surface roughness resulted in coating adhesion decrease. The data obtained in this work showed formal partial correspondence between treatment parameters and critical force value: an increase in the number of pulses led to both an increase in roughness and critical normal force.

The findings allowed to suggest that higher critical force values could be associated not with roughness and waviness increase, but mainly with the formation of an intermediate layer δ-TiN, the thickness of which increased with an increase in the number of pulses and a decrease in the density of absorbed energy.

Additional tests of samples treated at Q = 26 J/cm^2 were carried out. For this series of samples value of roughness parameters was decreased with the growth of number of pulses while value of Wa was slightly increased. The length of the track was 7.5 mm, the speed of moving sample was reduced by ~ 2 times. The test results are presented in Figure 6.

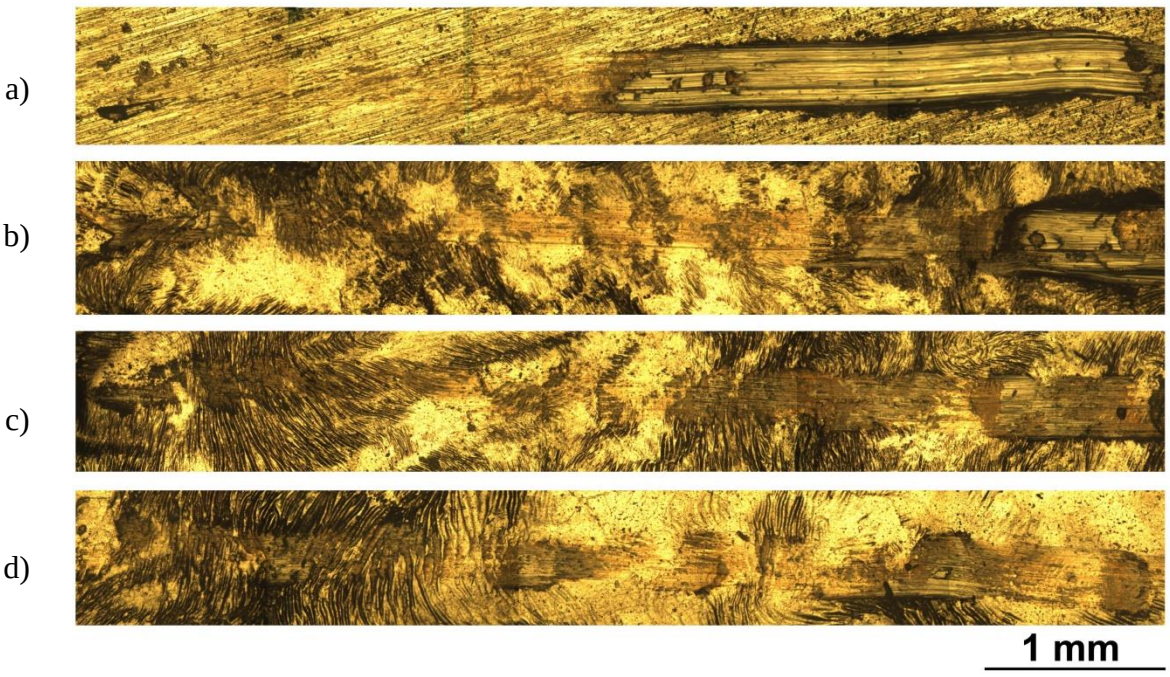

Figure 6. Optical microscopy images of scratch tracks on ZrN coated initial sample (a) and samples preliminary treated by CPF at Q=26 J/cm^2 with n=1 (b), n=3 (c) and n=6 (d) pulses.

According to the findings $Lc3^{max}$ for the untreated sample was equal to 71 N, for samples treated by CPF with one pulse - 125 N, treated by CPF with three pulses - 135 N. For the sample treated with 6 pulses no full removal of the coating was found at this testing mode. The value of $Lc3^{min}$ for all modes of plasma treatment was in the range of 100-110 N. Higher values of critical force in this test mode were associated with a decrease in a sample movement speed that would lead to a decrease in the shock loads applied to the surface asperities interacting with the indenter. Similar dependence of critical load on scratching speed was found in (Randall, 2019).

The findings showed that preliminary plasma treatment before ZrN coating deposition led to an increase in the value of the critical load Lc3. At the same time, the main factor that determines such a behavior is the formation of an intermediate layer of titanium nitride that grew during plasma processing. Bending cracks (the maximum stress is concentrated in the substrate) and

spallations (maximum stress is found in the area close to the coating/substrate interface) are considered to be the main mechanisms of hard coatings failure on ductile substrates during scratch tests (Zawischa et al., 2021). The failure mechanism is dependent on the *R/h* ratio, where *R*- radius of indenter tip and *h*- coatings thickness (Zawischa et al., 2021). High *R/h* ratio resulted in strong plastic deformation of the substrate and the coating failure due to formation of bending cracks. This failure mode should be observed at $R/h > 75$ according to results presented in (Zawischa et al., 2021). In our case $R/h=133$, thus one can expect appearance of bending cracks in the coating. So appearance of intermediate δ-TiN layer should impede appearance of bending cracks and may ~~be~~ stop their movement at δ-TiN layer interfaces. At the same time developed roughness did not allow to confirm this failure mode by optical microscopy investigations.

4. Conclusions

The findings showed that compression plasma flows treatment of Ti6Al-4V titanium alloy led to formation of more developed surface relief. Besides that formation of titanium nitride with a cubic crystal lattice was found at the surface.

Samples surface was coated by ZrN after preliminary plasma processing and scratch tests were carried out. It was found that for samples preliminary treated by plasma the track was characterized by the formation of several sequential local areas at which partial removal of the coating occurred and the last area, starting from which full coating removal was observed and the indenter interacted directly with the titanium alloy in the track. Continuous delamination of the coating along the edges of the track was observed just beginning from this area. The appearance of several such areas was associated with a developed surface after plasma impact.

Preliminary plasma processing provided a higher value of the critical force Lc3, which increased from 44 N (without processing) to 137 N (at the density of absorbed energy 26 J/cm^2, 6 pulses). A tendency of the critical force of Lc3 growth with a decrease in the density of absorbed energy and an increase in the number of pulses was found.

The analysis carried out allowed suggesting that higher critical force values were associated not with a change in roughness and waviness characteristics, but mainly with the formation of an δ-TiN intermediate layer, the thickness of which increased with an increase in the number of pulses and a decrease in the density of absorbed energy.

Acknowledgements

This work was supported financially by the Belarusian Republican Foundation for Fundamental Research (project no. T23RNF-228) and the Russian Science Foundation (project no. 23-49-10038).

References

Astashinski, V. M., Leyvi, A. Ya., Uglov, V. V., Cherenda, N. N., Yalovets, A. P., Formation of Relief on a Metallic Target Surface under the Action of Compression Plasma Flows. *Journal of Surface Investigation. X-ray, Synchrotron and Neutron Techniques*, vol. **8**, no 3, pp. 519–523, 2014.

Bazylev, B., Janeschitz, G., Landman, I., Loarte, A., Klimov, N.S., Podkovyrov, V.L., Safronov, V.M., Experimental and theoretical investigation of droplet emission from tungsten melt layer. *Fusion Engineering and Design*, vol. **84**, pp. 441-445, 2009.

Bruera, A., Puddu, P., Theimer, S., Villa-Vidaller, M., List, A., Bolelli, G., Gartner, F., Klassen, T., Lusvarghi, L., Adhesion of cold sprayed soft coatings: Effect of substrate roughness and hardness. *Surface and Coatings Technology*, vol. **466**, p. 129651, 2023.

Brunello, G., Brun, P., Gardin, C., Ferroni, L., Bressan, E., Meneghello, R., Biocompatibility and antibacterial properties of zirconium nitride coating on titanium abutments: An in vitro study. *PLoS ONE*, vol. **13**, no 6, p. e0199591, 2018.
Bull, S.J., EBerasetegui, G., An overview of the potential of quantitative coating adhesion measurement by scratch testing. *Tribology International*, vol. **39**, pp. 99–114, 2006.
Caraguay, S.J., Pereira, T.S., Cunha, A., Pereira, M., Xavier, F.A., The effect of laser surface textures on the adhesion strength and corrosion protection of organic coatings - Experimental assessment using the pull-off test and the shaft load blister test. *Progress in Organic Coatings*, vol. **180**, 107558, 2023.
Chen, H., Feng, R., Xia, T., Wen, Z., Li, Q., Qiu, X., Huang, B., Li, Y., Progress in Surface Modification of Titanium Implants by Hydrogel Coatings. *Gels*, vol. **9**, p. 423, 2023.
Chen, Q., Thouas, G. A., Metallic implant biomaterials. *Mater. Sci. Eng. R*, vol. **87**, pp. 1–57, 2015.
Cherenda, N., Leivi, A., Petukh, A., Uglov, V., Grigoriev, S., Vereschaka, A., Astashynski, V., Kuzmitski, A., Modification of Ti-6Al-4V titanium alloy surface relief by compression plasma flows impact. *High Temperature Material Processes*, vol. **28**, 2024. (in press, DOI: 10.1615/HighTempMatProc.2023050354)
Cherenda, N.N., Shimanskii, V. I., Uglov, V. V., Astashinskii, V. M., Ukhov, V. A., Nitriding of Steel and Titanium Surface Layers under the Action of Compression Plasma Flows. *Journal of Surface Investigation. X-ray, Synchrotron and Neutron Techniques*, vol. **6**, no. 2, pp. 319-325, 2012.
Cherenda, N.N., Uglov, V.V., Kuleshov, A.K., Astashynski, V.M., Kuzmitski, A.M., Surface nitriding and alloying of steels with Ti and Nb atoms by compression plasma flows treatment. *Vacuum*, **vol.** 129, pp. 170-177, 2016.
Chouirfa, H., Bouloussa, H., Migonney, V., Falentin-Daudré, C., Review of titanium surface modification techniques and coatings for antibacterial applications, *Acta Biomaterialia*, vol. **83**, pp. 37- 54, 2019.
Croll, S.G., Surface roughness profile and its effect on coating adhesion and corrosion protection: A review, *Progress in Organic Coatings*, vol. **148**, p. 105847, 2020.
Grabovetskaya, G. P., Stepanova, E. N., Zabudchenko O. V., Mishin, I. P., Formation of the Structure and Properties of the Near-Surface Layer in Alloys of the Ti–6Al–4V–H System Under Irradiation with a Pulsed Electron Beam, *Russian Physics Journal*, vol. 66, pp. 172–179, 2023.
Grigoriev, S., Vereschaka, A., Uglov, V., Milovich, F., Tabakov, V., Cherenda, N., Andreev, N., Migranov, M., Influence of the tribological properties of the Zr,Hf-(Zr,Hf)N-(Zr,Me,Hf,Al)N coatings (where Me is Mo, Ti, or Cr) with a nanostructured wear-resistant layer on their wear pattern during turning of steel. *Wear*, vol. **518-519**, p. 204624, 2023.
Herrera-Jimenez, E.J., Bousser, E., Schmitt, T., Klemberg-Sapieha, J.E., Martinu, L., Effect of plasma interface treatment on the microstructure, residual stress profile, and mechanical properties of PVD TiN coatings on Ti-6Al-4V substrates, *Surf. Coat. Technol.*, vol. **413**, p. 127058, 2021.
Hong, Q., Wang, S., Yin, S., Influence of atmospheric pressure plasma modification on surface properties of aluminum alloy substrate and its interfacial adhesion strength with electrodeposited nickel coating. *Surface & Coatings Technology*, vol. **474**, p. 130050, 2023.
Kaur, M., Singh, K., Review on titanium and titanium based alloys as biomaterials for orthopaedic applications. *Materials Science & Engineering C*, vol. **102**, pp. 844-862, 2019.
Krasnikov, V.S., Leivy, A.Y., Mayer, A.E., Yalovets, A.P., Surface microrelief smoothing mechanisms in a target irradiated by an intense charged particle beam, *Rus. J. Tech. Physics*, vol. **52**, no. 4, p. 431, 2007.
Kumar, A., Mulik, R., S., Improving tribological behavior of titanium nitride (TiN) hard coatings via zirconium (Zr) or vanadium (V) doping, *Tribology International*, vol. **189**, p. 108997, 2023.

Kurup, A., Dhatrak, P., Khasnis, N., Surface modification techniques of titanium and titanium alloys for biomedical dental applications: A review, *Materials Today: Proceedings*, vol. **39**, no 1, pp. 84-90, 2021.
Leroch, S., Eder, S.J., Varga, M., Ripoll, M.R., Material point simulations as a basis for determining Johnson–Cookvhardening parameters via instrumented scratch tests. *International Journal of Solids and Structures*, vol. **267**, p. 112146, 2023.
Liu, K., Jin, Z., Zakharova, N., Zeng, L., Haghshenas, M., Adeyilola, A., Saurabh, S., Comparison of shale fracture toughness obtained from scratch test and nanoindentation test. *International Journal of Rock Mechanics & Mining Sciences*, vol. **162**, p. 105282, 2023.
Lu, A., Gao, Y., Jin, T., Luo, X., Zeng, Q., Shang, Z., Effects of surface roughness and texture on the bacterial adhesion on the bearing surface of bio-ceramic joint implants: An in vitro study, *Ceramics International*, vol. 46, pp. 6550-6559, 2020.
Nouri, A., Wen C,. Introduction to surface coating and modification for metallic biomaterials, in *Surface Coating and Modification of Metallic Biomaterials*, C. Wen, Ed., Cambridge: Woodhead Publishing, pp. 3-60, 2015.
Randall, N.X., The current state-of-the-art in svratch testing of coated systems, *Surface and Coatings Technology*, vol. **380**, p. 125092, 2019.
Robles, D., Brizuela, A., Fernández-Domínguez, M., Gil, J., Corrosion Resistance and Titanium Ion Release of Hybrid Dental Implants, *Materials*, vol. **16**, p. 3650, 2023.
Simões, I. G., Reis, A. C., Valente, M. L. C., Influence of surface treatment by laser irradiation on bacterial adhesion on surfaces of titanium implants and their alloys: Systematic review, *The Saudi Dental Journal*, vol. **35**, no 2, pp. 111-124, 2023.
Sachin, P.G., Uppoor, A.S., Nayak, S.U., Nano-scale surface modification of dental implants – An emerging boon for osseointegration and biofilm, *Control Acta Marisiensis - Seria Medica*, vol. **68**, no 4, pp. 154-158, 2022.
Tahir, A., Li, G., Liu, M., Yang, G., Li, C., Wang, Y., Li, C., Improving WC-Co coating adhesive strength on rough substrate: Finite element modeling and experiment. *Journal of Materials Science & Technology*, vol. **37**, pp. 1-8, 2020.
Takadoum, J., Bennani, H. H. Influence of substrate roughness and coating thickness on adhesion, friction and wear of TiN films, *Surface and Coatings Technology*, vol. **96**, pp. 272-282, 1997.
Tardelli, J. D. C., Firmino, A. C. D., Ferreira, I., Reis A.C., Influence of the roughness of dental implants obtained by additive manufacturing on osteoblastic adhesion and proliferation: A systematic review, *Heliyon*, vol. **8**, no 12, p. e12505, 2022.
Uglov, V.V., Anishchik, V.M., Astashynski, V.V., Stalmoshenok, E.K., Rusalsky, D.P., Cherenda, N.N., Rumyanceva, I.N., Askerko, V.V., Kuz'mitski, A.M., Structure-phase transformation of high speed steel by various high intensity ion-plasma treatments. *Surface and Coatings Technology*, vol. **180–181**, pp. 108-112, 2004.
Ul-Hamid, A., Synthesis, microstructural characterization and nanoindentation of Zr, Zr-nitride and Zr-carbonitride coatings deposited using magnetron sputtering. *Journal of Advanced Research*, vol. **29**, pp. 107–119, 2021.
Varga, M., Ventura Cervellón, A.M., Leroch, S., Eder, S.J., Rojacz, H., Ripoll, M. R., Fundamental abrasive contact at high speeds: Scratch testing in experiment and simulation. *Wear*, vol. **522**, p. 204696, 2023.
Vereschaka, A., Aksenenko, A., Sitnikov, N., Migranov, M., Shevchenko, S., Sotova, C., Batako, A., Andreev, N., Effect of adhesion and tribological properties of modified composite nanostructured multi-layer nitride coatings on WC-Co tools life, *Tribology International*, vol. **128**, pp. 313–327, 2018.
Vereschaka, A., Tabakov, V., Grigoriev, S., Sitnikov, N., Milovich, F., Andreev, N., Sotova, C., Kutina, N., Investigation of the influence of the thickness of nanolayers in wear-resistant layers of Ti-TiN-(Ti,Cr,Al)N coating on destruction in the cutting and wear of carbide cutting tools. *Surf. Coat. Technol*., vol. **385**, p. 125402, 2020.

Wang, Q., Zhou, P., Liu, S., Attarilar, S., Ma, R. L.-W., Zhong Y., Wang, L., Multi-Scale Surface Treatments of Titanium Implants for Rapid Osseointegration: A Review, *Nanomaterials*, vol. **10**, p. 1244, 2020.

Ward, L.P., Stratford, K.N., Subramanian, C. and Wilks, T.P., Observations on the structure, hardness and adhesion properties of a selection of multicomponent refractory element nitride coatings. *Journal of Materials Processing Technology*, vol. **56**, pp. 375-384, 1996.

Wu, N., Gao, H., Wang, X., Pei, X. Surface Modification of Titanium Implants by Metal Ions and Nanoparticles for Biomedical Application, *ACS Biomater. Sci. Eng.*, vol. **9**, no 6, pp. 2970–2990, 2023.

Zawischa, M., Supian, M., Makowski, S., Schaller, F., Weihnacht, V., Generalized approach of scratch adhesion testing and failure classification for hard coatings using the concept of relative area of delamination and properly scaled indenters. *Surface & Coatings Technology*, vol. **415**, p. 127118, 2021.

Zhang, J., Li, Y., Zheng, X., Wang, G., Zhao, M., Determination of plastic properties of surface modification layer of metallic materials from scratch tests. *Engineering Failure Analysis*, vol. **142**, p. 106754, 2022.

Zhao, X., Wang, B., Lai, W., Zhang, G., Zeng, R., Li, W., Wang, X., Improved tribological properties, cyto-biocompatibility and anti-inflammatory ability of additive manufactured Ti-6Al-4V alloy through surface texturing and nitriding. *Surface & Coatings Technology*, vol. **425**, p. 127686, 2021.

Table 1. Roughness and waviness parameters of Ti-6Al-4V alloy surface after CPF treatment at different Q and n (Cherenda et al., 2024).

Relief parameter	Q=26 J/cm^2			Q=30 J/cm^2			Q=37 J/cm^2		
	n=1	n=3	n=6	n=1	n=3	n=6	n=1	n=3	n=6
R_a, μm	1.40	1.44	1.19	0.73	1.79	2.21	1.25	1.41	2.74
R_z, μm	9.51	9.59	6.28	5.78	11.79	11.89	8.10	10.46	16.28
W_a, μm	1.51	2.37	2.85	1.42	2.97	4.36	2.38	2.86	4.40

Table 2. Average critical normal force Lc3 for delamination of ZrN coating from initial Ti-6Al-4V sample and samples preliminary treated by CPF (track length 15 mm).

<Lc3>	Initial	26 J/cm^2			30 J/cm^2			37 J/cm^2		
		n=1	n=3	n=6	n=1	n=3	n=6	n=1	n=3	n=6
$Lc3^{min}$, N	44	60	79	79	37	57	47	34	31	44
$Lc3^{max}$, N	44	111	128	137	65	115	100	81	88	87